Growth mechanism of carbon nanotube forests by chemical vapor deposition

Oleg A. Louchev,[a] Yoichiro Sato, and Hisao Kanda
Advanced Materials Laboratory, National Institute for Materials Science, 1-1 Namiki, Tsukuba, Ibaraki 305-0044, Japan

(Received 10 December 2001; accepted for publication 8 February 2002)

Analysis of kinetics processes involved in carbon nanotube (NT) forest growth during chemical vapor deposition suggests that: (i) carbon species are unable to penetrate to the forest bottom whenever the mean free path in gas is much larger than the typical distance between NTs; instead they collide with NT surfaces, chemisorbing within the top few microns, diffuse along the surface, and feed the growth at nanotube tips, (ii) wherever a catalyst nanoparticle is present, at the substrate or on the nanotube tip, in the postnucleation stage its role in feeding NT growth by C dissolution and bulk diffusion is negligibly small in comparison with the surface diffusion of C species adsorbing on the lateral surface of nanotubes, and (iii) bulk diffusion of C through the catalyst nanoparticle, defining the characteristic times of C penetration to nanoparticle base and surface saturation with C, is shown to play a major role in selection of the initial mode of nanotube nucleation and growth.
 [DOI: 10.1063/1.1468266]

Growth of well aligned C nanotube (NT) forests by chemical vapor deposition (CVD) on preformed catalyst nanoparticle arrays represents an effective technique for NT production, and has been studied by several groups trying to optimize the parameters of this process for production of cold electron emitters and other applications.[1–6] When interpreting their results, the majority of above reports refer to the model of NT growth by continuous C diffusion through the metal nanoparticle catalyzing NT growth,[7–9] regardless of where catalyst nanoparticles are found, on the NT tips or the substrate. The aim of this letter is twofold: first, to provide an order of magnitude analysis of the growth kinetics involved in CVD carbon NT forest growth, outlining major contradictions which arise in the application of the aforementioned model for a particular experimental study with Fe catalyst arrays,[6] and, second, to suggest another NT forest growth mechanism which is responsible for CVD growth in many practically important cases.

Let us consider the parameters of an NT forest rooted at the Fe nanoparticles array (see Fig. 1). The analysis of the transport phenomena in the gas phase involved in the experiments[6] shows that the diffusion of C through the nanoparticles remaining at the substrate may not be involved in the latest stages of NT forest growth. That is, to reach Fe nanoparticles remaining on the substrate, C species should penetrate through the forest. This appears to be impossible in view of the typical free mean path in the gas given by:

$$l_g = k_B T/(\sqrt{2}\sigma P) \approx 30-50\ \mu\text{m}, \tag{1}$$

for operational pressure $P=20$ Torr and $T=600-1000$ K,[6] ($\sigma \cong 10^{-19}$ m^2) which is much higher than the intertube distance within the forest, $\cong 1/\sqrt{N} \cong 1\ \mu$m (for tube surface density $N \cong 10^8$ cm^{-2}). That is, inside the forest ballistic mass transfer takes place in which gas species collide only with NTs without diffusion along the intertube space to the substrate. An estimate of the ballistic integral for profiled interfaces[10] taking into account forest intertube distance ($\cong 1\ \mu$m) and NT diameter ($\cong 0.1\ \mu$m),[6] shows that species impinging into the forest (up to $\approx 100\ \mu$m in height) collide with NTs within a distance of $\approx 10\ \mu$m from the top. The forest bottom is reached only by a negligibly small number of species impinging within a much smaller solid angle, $\delta\Omega_1$, than the solid angles for impinging on a NT top, $\delta\Omega_2$ (see Fig. 1). The NT surface represents a deep energy well for C species, ≈ 1.8 eV (Ref. 11) for interaction with C (CH_3) and obviously more for C_2H_2. Therefore, CH_3 and C_2H_2 units present in plasma or thermally excited gas[12] are

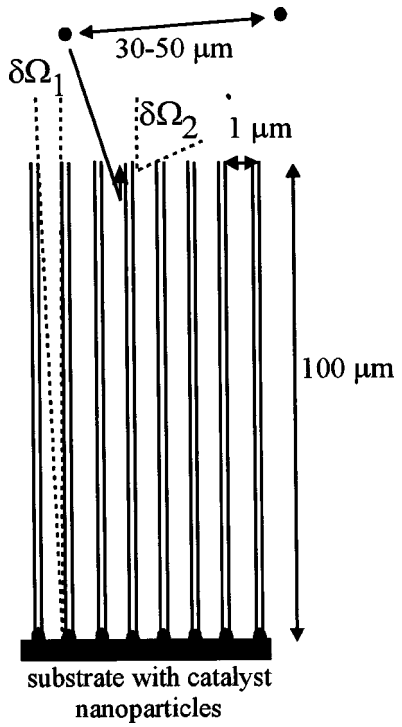

FIG. 1. Sketch of carbon NT forest with parameters (related to Ref. 6).

[a]Electronic mail: louchev.oleg@nims.go.jp

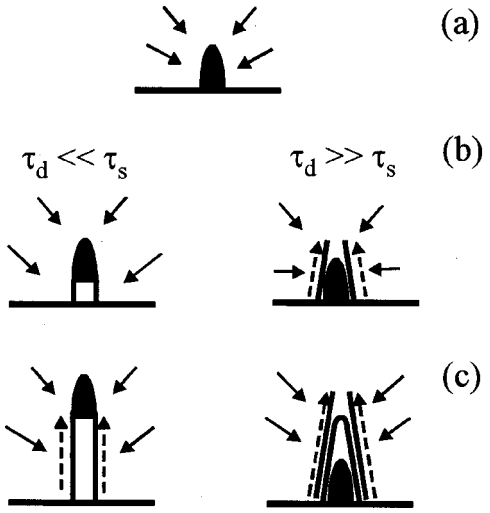

FIG. 2. Sketch of the proposed selection mechanism defining whether the nanoparticle is detached from the substrate on the NT tip, catalyzing growth and preventing NT closure (left-hand side) or remains on the substrate serving as an initial template for NT nucleation (right-hand side): (a) stage of nanoparticle saturation with carbon, (b) stage of NT nucleation, and (c) stage of postnucleation growth. Solid and dashed arrows indicate carbon flux from vapor and surface diffusion fluxes, respectively.

captured by collisions on the NT surface within the top few microns, and are unable to penetrate to the forest bottom. Let us also note that if one assumes that NT growth occurs via C incorporation at the NT base on the substrate an additional serious contradiction appears as to why the top part of NTs subject to significantly larger C fluxes remain uncovered by any kind of C deposit, i.e., graphite or amorphous carbon, which are well known to appear in C film growth in plasma assisted CVD using CH_4. Instead, assuming growth at the upper tips and nonpenetration of C species to the forest bottom, one can understand why the bottom part of forest remains unfilled by any kind of C deposit.

Let us additionally consider the growth of a NT rooted at the catalyst nanoparticle subject to C flux from gas. Analysis of the diffusion process shows that, for an individual NT, the contribution of C dissolution and diffusion through the catalyst nanoparticle in feeding NT growth is restricted by the initial stage of NT growth, i.e., when the particle cools down causing C precipitation from the supersaturated particle and NT nucleus formation. The role of this mechanism in the further postnucleation stage of NT growth becomes negligibly small in comparison with the contribution of the surface diffusion (SD) of C species along the NT surface. In effect, C atoms are found to have large adsorption energy for the NT surface, $E_a \approx 1.8$ eV, and a low activation energy of SD, $\delta E_D \approx 0.13$ eV.[11] Thus, the growth of NTs may be fed by C species chemisorbed on a NT surface over micronscale surface diffusion lengths defined by:

$$\lambda_D = 2(D_s \tau_a)^{1/2} = 2a_0 \exp[(E_a - \delta E_D)/2k_B T], \tag{2}$$

where $\tau_a \cong v^{-1} \exp(E_a/k_B T)$ is the adsorption time and the SD coefficient, D_s, is given by:

$$D_s \cong a_0^2 v \exp(-\delta E_D/k_B T), \tag{3}$$

where $v = (1-3) \times 10^{13}$ Hz is the vibration frequency and a_0 is the intersite distance.

For a NT rooted at a metal nanoparticle exposed to C flux from gas, $Q = P_c/(2\pi m k_B T)^{1/2}$, the total C flux onto the particle surface is $\cong Q \psi \pi R_P^2$, where R_p is the particle radius and ψ is a factor which takes into account the part of the particle surface subject to the C flux (ψ varies from 2, for NT radius $R \cong R_p$ to 4, for NT radius $R \ll R_p$). The flux of C onto the NT surface, feeding growth by SD is $\cong Q 2\pi RL$, where L is the current length of the NT. The contribution of SD prevails when $2RL \gg \psi R_p^2$. Remembering that NTs are typically rooted on particles with diameters close to those of the NTs, i.e., $R \cong R_p$ and $\psi \cong 2$, one finds that SD is significant even for $L \cong R_p$, and prevails when $L \gg R_p$. The effect of SD appears even more significant if one compares D_s with that of C bulk diffusion in Fe:[12,13]

$$D_b \cong D_0 \exp(-\delta E_b/k_B T), \tag{4}$$

where $D_0 \approx 0.1-0.5$ cm^2/s and $\delta E_b \approx 137-153$ kJ/mol ($\approx 1.4-1.6$ eV) for $T = 1000-1500$ K. For $T = 1500$ K, $D_s \approx 1.5 \times 10^{-3}$ cm^2/s is about 3 orders of magnitude higher than that of C diffusion into Fe, $D_b \approx (1-2) \times 10^{-6}$ cm^2/s. For $T = 1000$ K, $D_s \approx 10^{-3}$ cm^2/s $\gg D_b \approx 10^{-8}$ cm^2/s. Even for liquid metal $D_b \approx (1-5) \times 10^{-5}$ cm^2/s (Ref. 13) $\ll D_s$. Additionally, if we consider the case of NT forest growth on nanoparticles embedded into mesoporous silica[1] it is difficult to imagine how NTs may grow via the mechanism of C precipitation from Fe because in this case C has to diffuse additionally through the silica.

These estimates show that, independent of whether the nanoparticle is located at the NT base or on the upper tip, in the postnucleation stage NT forest growth proceeds via the C incorporation into the NT tip fed by surface diffusion over the lateral surface, including also the stages of dehydrogenation of chemisorbed hydrocarbons. However, the diffusion process through the nanoparticle is important for NT nucleation stage and also for selection of the NT growth mode, schematized in Fig. 2, defining whether the nanoparticle remains at the substrate, or on the tip of the growing NT. We suggest here that this selection is defined by two characteristic times, dependent on D_b: (i) the diffusion time of order:

$$\tau_d \approx R_p{}^2/D_b, \tag{5}$$

required for C penetration to the nanoparticle base, and (ii) the surface saturation time of order:[14]

$$\tau_s \approx C^{*2} D_b/Q^2. \tag{6}$$

corresponding to the increase of C content to the saturation concentration, C^*, triggering C precipitation directly on the upper surface of nanoparticle.

If $\tau_d \gg \tau_s$, the nanoparticle surface saturates with C much faster than C penetrates to its base, and, therefore, C precipitates at the nanoparticle surface which provides a nanoscale template for NT nucleation. In contrast, when $\tau_d \ll \tau_s$ C penetrates to the base much faster than the nanoparticle surface reaches saturation threshold, and C precipitates at the bottom, lifting the nanoparticle, and later on maintaining it on the NT tip. In this mode, the role of the nanoparticle remains important for inhibiting pentagon formation and preventing NT tip closure. This scenario is supported by number estimates for typical conditions, $T = 1000$ K and $P_c \approx 20$ Torr,[6] giving $Q \approx 10^{22}$ l/cm^{2}s and including nanopar-

ticle radius, which defines melting temperature.[15] That is, the value of D_b depends on the nanoparticle state, and an Fe nanoparticle with $R_p<3$ nm remains liquid due to the capillary effect[15] with $D_b\approx10^{-5}$ cm^2/s whereas for $R_p>3$ nm, the nanoparticle is solid with $D_b\approx10^{-8}$ cm^2/s. Fe saturates at ≈10–20 at. % of C and $C^*\approx10^{22}$ cm^{-3}. Hence, for a nanoparticle of $R_p=10$ nm, $\tau_d\approx10^{-4}$ s$\gg\tau_s\approx10^{-8}$ s meaning that its surface saturates much faster than C penetrates to its base. Surface saturation with C isolates the nanoparticle from further C penetration leading to C precipitation, NT nucleation and growth on the upper surface of the nanoparticle. In contrast, for a liquid nanoparticle of $R_p=1$ nm, $\tau_d\approx10^{-9}$ s$\ll\tau_s\approx10^{-5}$ s, meaning that C precipitates and the NT starts to grow at the nanoparticle bottom because of more favorable conditions for conductive heat dissipation into the substrate. This mode has some additional restrictions. First, the diffusion time, τ_d, should also be much smaller than the characteristic repetition time,

$$\tau_{\text{imp}}\approx 1/(Qa_0^2), \tag{7}$$

with which C impinges into the nanoparticle (where a_0 is the interatomic distance). Otherwise, the C surface concentration increases, leading finally to C precipitation on the surface. At $T=1000$ K and $Q\approx10^{22}$ l/cm^2 s for a Fe nanoparticle of $R_p=1$ nm $\tau_{\text{imp}}\approx10^{-6}$ s$\gg\tau_d\approx10^{-9}$ s, and, hence, the nanoparticle can remain uncovered by C on the NT tip during growth. By contrast, for a Fe nanoparticle of $R_p=10$ nm $\tau_{\text{imp}}\approx10^{-6}$ s$\ll\tau_d\approx10^{-4}$ s, and the nanoparticle lifted up to the NT tip will be covered with time by C. Second, the possibility of nanoparticle lifting depends also on whether the energy gain, resulting from C transition from the nanoparticle into the NT ring nucleus, is sufficient to overcome the interface energy between nanoparticle and substrate, $\approx\gamma R_p{}^2$ (γ is the interface energy per unit area). Lifting a solid particle from the substrate requires breaking strong nanoparticle–substrate interface bonds, whereas the liquid particle is bound to the substrate by a significantly weaker interaction. In this mode, the growth may be fed by C diffusion through the catalyst particle in the postnucleation stage,[7–9] however, the contribution of SD of C impinging into the NT surface becomes dominant when its length $L\gg R_p$. It is worth adding here that in the interaction with a forming NT the nanoparticle is able to change its initial form in order to minimize the surface energy.[16] Eventually solidifying, it may also become faceted or cylindrical, conforming to the internal surface of the NT.[16] Nanoparticles may also be present at both ends of the NT, providing a nanoscale template for NT nucleation and inhibiting pentagon formation at the NT growth tip. Such a situation is probably limited to specific cases such as NT growth by pyrolysis of iron phthalocyanine,[17] where Fe is involved in codeposition with C during the postnucleation stage as well.

This selection mechanism for NT forest growth modes defines the final morphology of NTs and their properties. The nanoparticle held on the NT tip inhibits the formation of pentagons and consequent NT closure, and allows growth of straight wall NTs. A nanoparticle remaining at the NT base provides only an initial template with nanoscale curvature for NT nucleation predefining the morphology of resulting NTs. Cylindrical nanoparticles are able to form NTs with a straight wall whereas on conical nanoparticles, conical NT nuclei tend to form leading to growth of bamboo-like NTs.[6] The formation of ''bamboo''-like structures in the CVD process may be attributed to the periodic closure and subsequent nucleation of the next conical multilayer wall (Fig. 2). There are two slightly distinct scenarios of bamboo-like growth. In the first scenario, similar to that of Refs. 18 and 19, the increase in the first multilayer wall length (i) provokes an increase of surface concentration which triggers surface nucleation. The second multilayer wall, fed by SD from both sides of the growth edge, (ii) has a larger growth rate, catches up with the underling wall and inhibits its growth, and (iii) makes it close up. The simulation of bamboo-like growth in physical vapor deposition (PVD)[18,19] is in qualitative agreement with experimental data on the interbamboo layer distance in CVD grown NTs as a function of T, in spite of the existence of differences between PVD and CVD growth. That is, the interbamboo layer distance increases from ≈30 nm for $T\approx1000$ K to about ≈80 nm for $T\approx1200$ K.[6] For bamboo-like growth simulation in PVD mode, the interbamboo layer distance is ≈1–2 nm for $T=1100$ K and ≈10–20 nm for $T=1400$ K (Figs. 3 and 7 of Ref. 19)—showing the same tendency with increase in T. In the second scenario, the first NT bamboo layer grows until its closure due to the predefined conical shape. After the closure, the surface sink for C is cut off, and the surface concentration of C species increases and triggers the nucleation of the new bamboo layer which grows until its own closure, provoking once again layer nucleation.

[1] W. Z. Li, S. S. Xie, L. X. Qian, B. H. Chang, B. S. Zou, W. Y. Zhou, R. A. Zhao, and G. Wang, Science **274**, 1701 (1996).
[2] M. Terrones, N. Grobert, J. Olivares, J. P. Zhang, H. Terrones, K. Kordatos, W. K. Hsu, J. P. Hare, P. D. Townsend, K. Prassides, A. K. Cheetham, H. W. Kroto, and D. R. M. Walton, Nature (London) **388**, 52 (1997).
[3] Z. F. Ren, Z. P. Huang, J. W. Xu, J. H. Wang, P. Bush, M. P. Siegal, and P. N. Provencio, Science **282**, 1105 (1998).
[4] S. Fan, M. G. Chapline, N. R. Franklin, T. W. Tombler, A. M. Cassell, and H. Dai, Science **283**, 512 (1999).
[5] Z. F. Ren, Z. P. Huang, D. Z. Wang, J. G. Wen, J. W. Xu, J. H. Wang, L. E. Calvet, J. Chen, J. F. Klemic, and M. A. Reed, Appl. Phys. Lett. **75**, 1086 (1999); H. Ago, T. Komatsu, S. Ohshima, Y. Kuriki, and M. Yumura, *ibid.* **77**, 79 (2000); C. Bower, W. Zhu, S. Jin, and O. Zhou, *ibid.* **77**, 830 (2000); Z. W. Pan, S. S. Xie, B. H. Chang, L. F. Sun, W. Y. Zhou, and G. Wang, Chem. Phys. Lett. **299**, 97 (1999); C. K. Lee and J. Park, J. Phys. Chem. B **105**, 2365 (2001).
[6] H. Cui, O. Zhou, and B. R. Stoner, J. Appl. Phys. **88**, 6072 (2000).
[7] A. Oberline, M. Endo, and T. Koyama, J. Cryst. Growth **32**, 335 (1976).
[8] R. T. K. Baker and P. S. Harris, in *Chemistry and Physics of Carbon*, edited by P. L. Walker, Jr. and P. A. Thrower (Marcel Dekker, New York, 1978), pp. 83–161.
[9] G. G. Tibbetts, J. Cryst. Growth **66**, 632 (1984).
[10] O. A. Louchev, Y. Sato, and H. Kanda, J. Appl. Phys. **89**, 2115 (2001).
[11] Y. H. Lee, S. G. Kim, and D. Tomanek, Phys. Rev. Lett. **78**, 2393 (1997).
[12] W. L. Hsu, J. Appl. Phys. **72**, 3102 (1992).
[13] *Physical Properties* (*Fizicheskie vellichini, in Russian*), edited by I. S. Grigoriev and E. Z. Meilikhov (Moscow, Energoatomizdat, 1991); H. M. Strong and R. E. Hanneman, J. Chem. Phys. **46**, 3668 (1966).
[14] O. A. Louchev, C. Dussarat, and Y. Sato, J. Appl. Phys. **86**, 1736 (1999).
[15] Melting temperature, T_m, is defined by: $T_m=T_{m0}\exp(-\gamma K/\Delta H)$, where T_{m0} is the melting temperature of the flat surface, $\gamma\approx2$ J/m^2 is the surface tension of Fe, ΔH is the latent heat per volume unit, and $K=1/\rho_1+1/\rho_2$ is the curvature with ρ_1 and ρ_2 as the main radii of curvature.
[16] L. T. Chadderton and Y. Chen, J. Cryst. Growth (submitted).
[17] S. Huang, L. Dai, and A. W. H. Mau, J. Mater. Chem. **9**, 1221 (1999).
[18] O. A. Louchev and Y. Sato, Appl. Phys. Lett. **74**, 194 (1999).
[19] O. A. Louchev, Y. Sato, and H. Kanda, J. Appl. Phys. **89**, 3438 (2001).